a

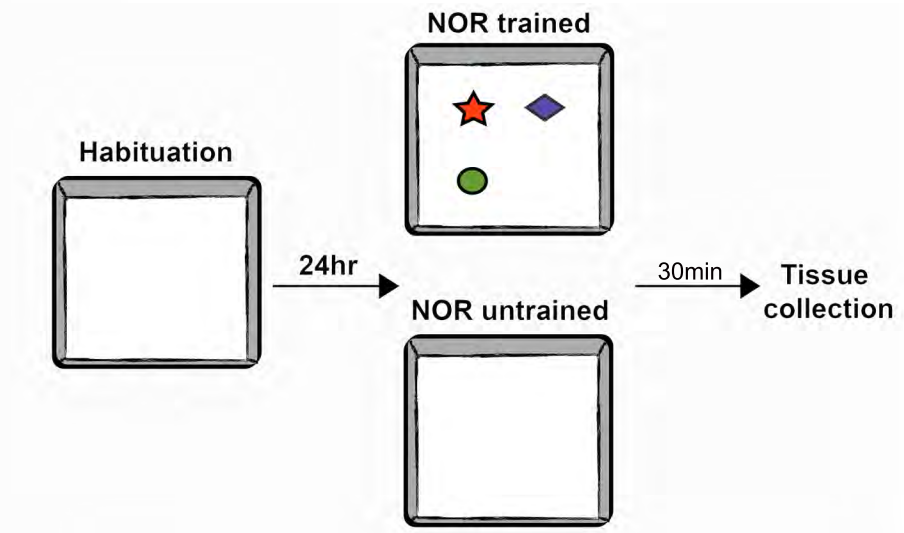

b

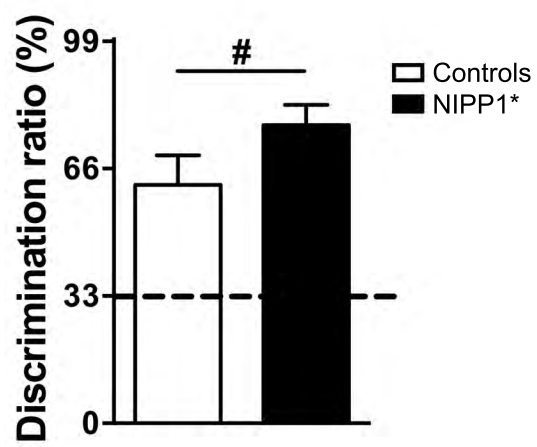

Supplementary Figure 1: NOR training of mice before deep sequencing screening. (a) Experimental set-up for NOR training conducted prior to deep sequencing. (b) Performance of animals used for sequencing tested 5min after training, expressed as discrimination ratio. Both groups demonstrated significant discrimination of novel object (chance level set at 33%) (one-sample t-test, control: $t_5=4.589$, $p<0.01$; NIPP1*: $t_5=8.525$, $p<0.001$) but NIPP1* mice had better performance than controls (unpaired t test between controls and NIPP1*: $t_{10}=1.93$, #$p=0.08$). Controls, n=6; NIPP1*, n=6. Bar graphs represent mean ± s.e.m.

a

Insert range	Matching to genome (%)	Matching to miRNA (%)
19 - 26	96.9	92.1
19 - 44	94.7	82.9
27 - 44	66.3	0.1

b

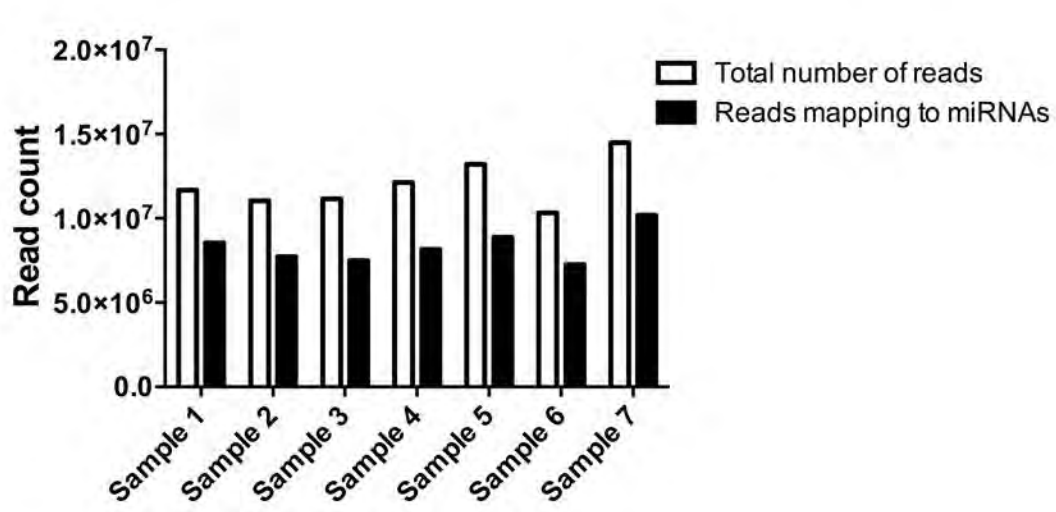

c

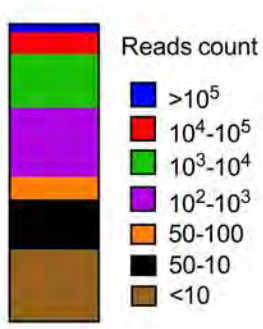

d

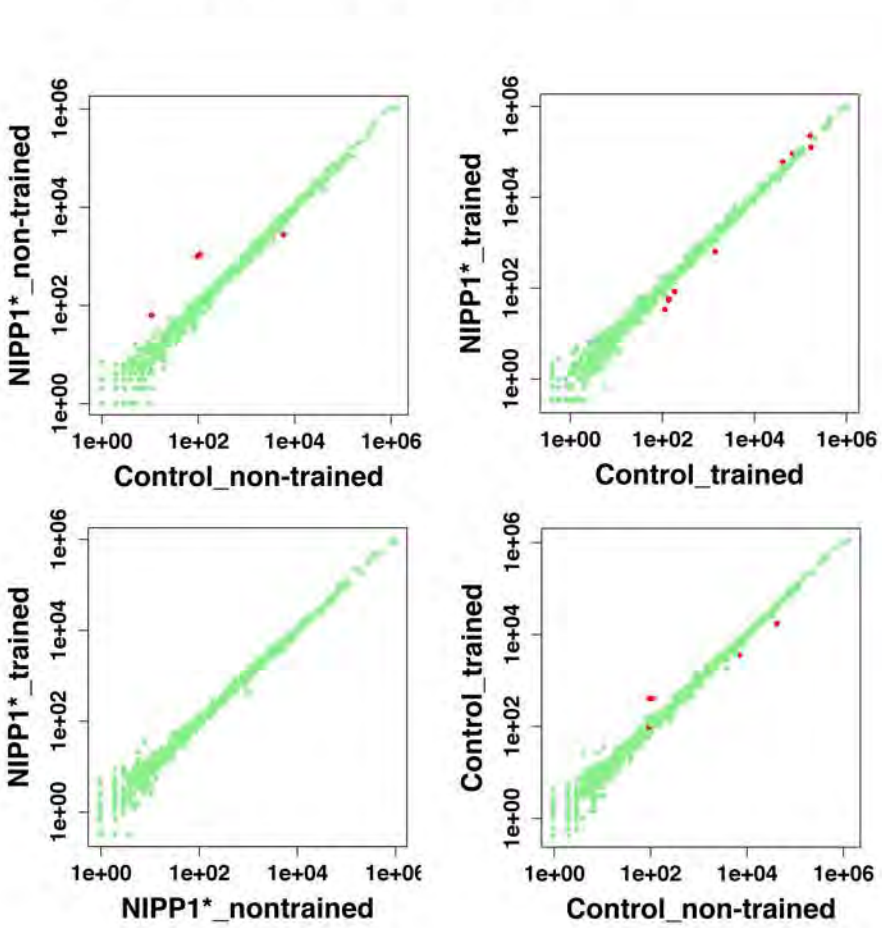

Supplementary Figure 2: Distribution of reads obtained by deep sequencing and correlation between groups. (a) Proportion of sequence reads mapping to the genome and known miRNAs. (b) Comparison of number of reads that uniquely map to miRNAs in each sample (c) Average distribution of all identified miRNAs based on reads count expressed as ‘read counts’. (d) Correlation of expression level of all identified miRNAs (each represented as a dot in ln(read count))) between the different experimental groups (NIPP1* and control littermates, trained or untrained). Red dots represent differentially expressed miRNAs (adjusted $p<0.05$).

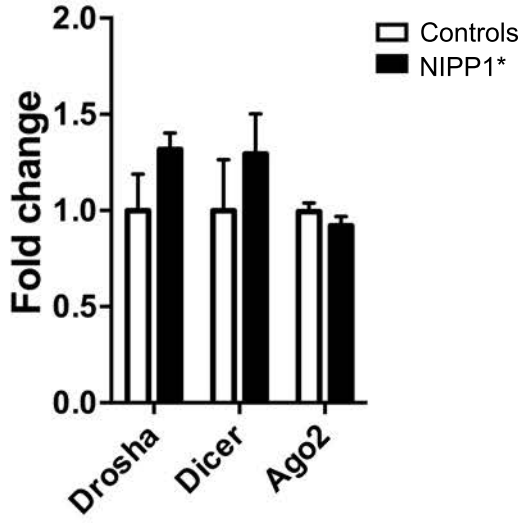

Supplementary Figure 3: qPCR quantification of major components of the miRNA biogenesis machinery in NIPP1* and control mice. Drosha: t8=1.54, p=0.16; Dicer: t8=0.89, p=0.40; Ago2: t8=1.10, p=0.30; Controls, n=5; NIPP1*, n=5. Bar graphs represent mean ± s.e.m.

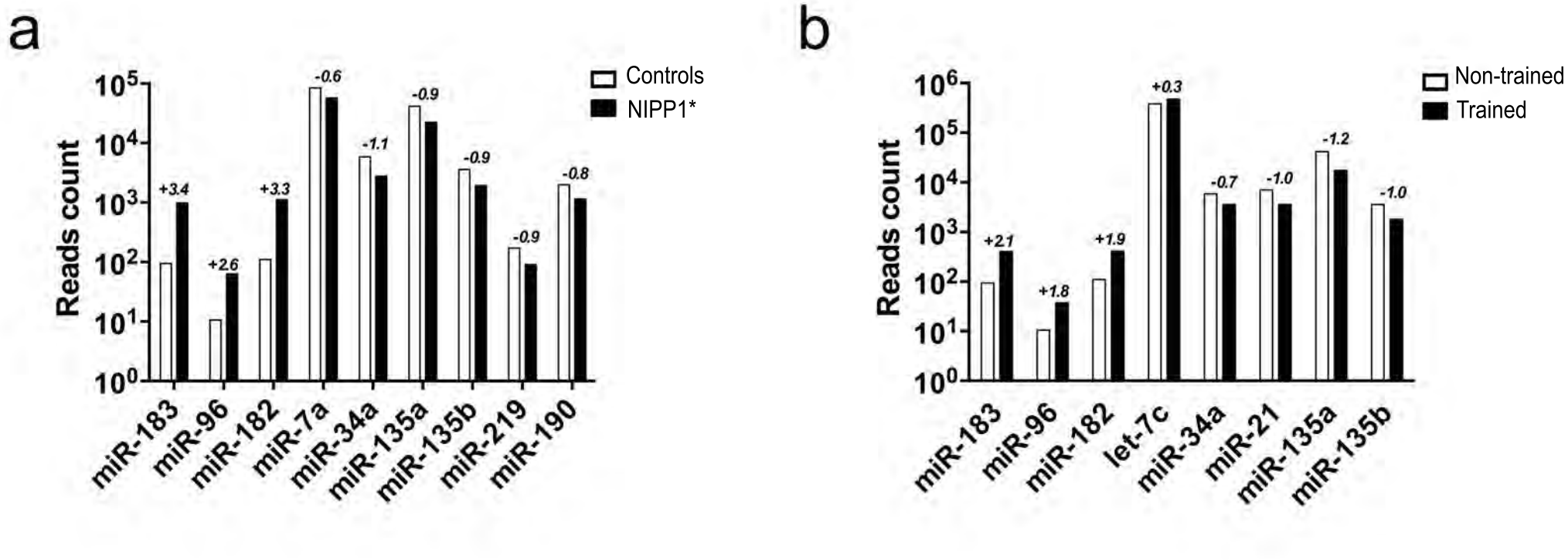

Supplementary Figure 4: Relative abundance of differentially expressed miRNAs based on reads count per million (log 2). (a) NIPP1* compared to control mice; (b) trained controls compared to non-trained controls. The number above bars indicates fold change between groups.

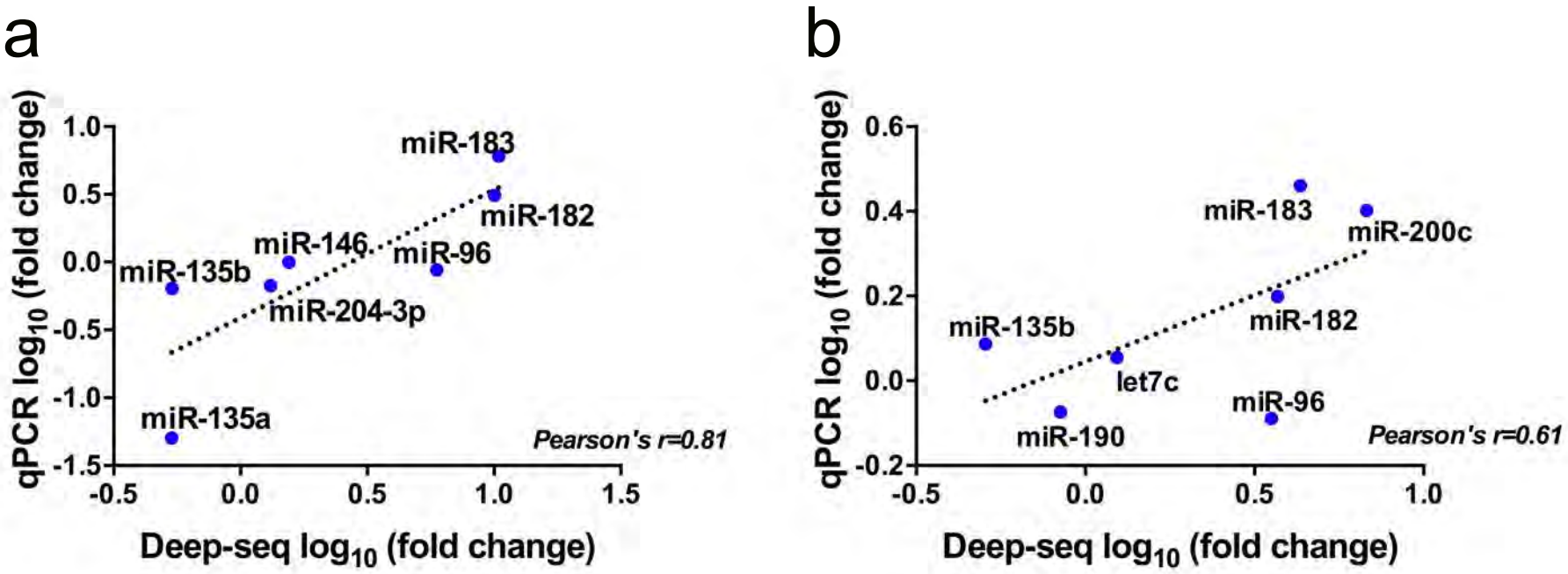

Supplementary Figure 5: Correlation between deep sequencing and qPCR-based quantification of miRNAs differentially expressed: (a) in NIPP1* and control mice; (b) in NOR-trained and untrained mice.

a

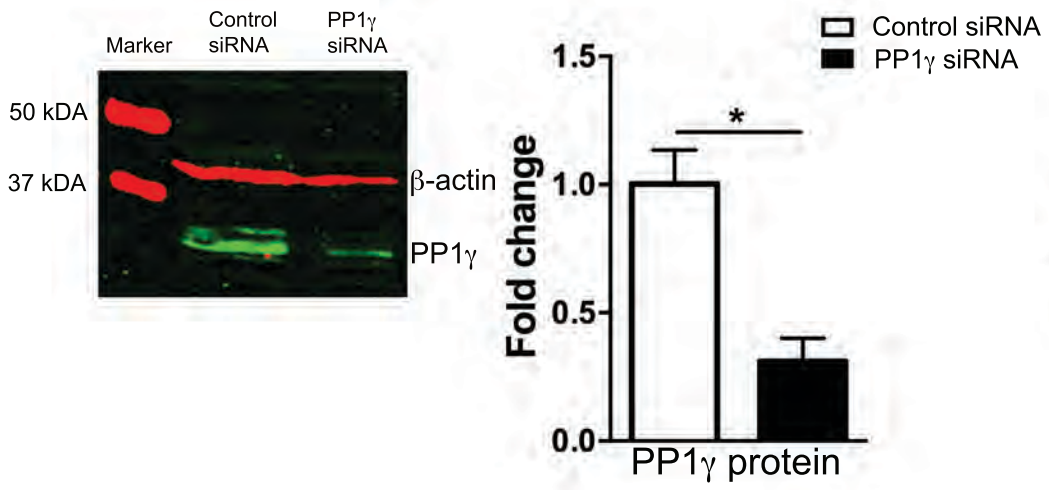

b

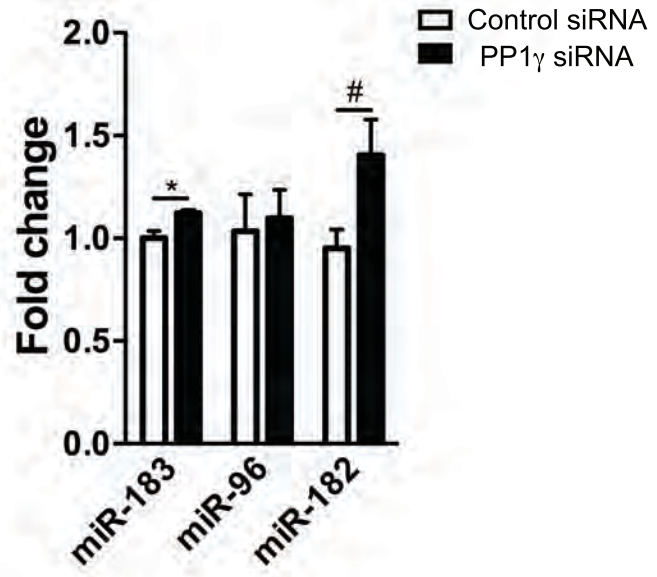

c

Whole cell extract

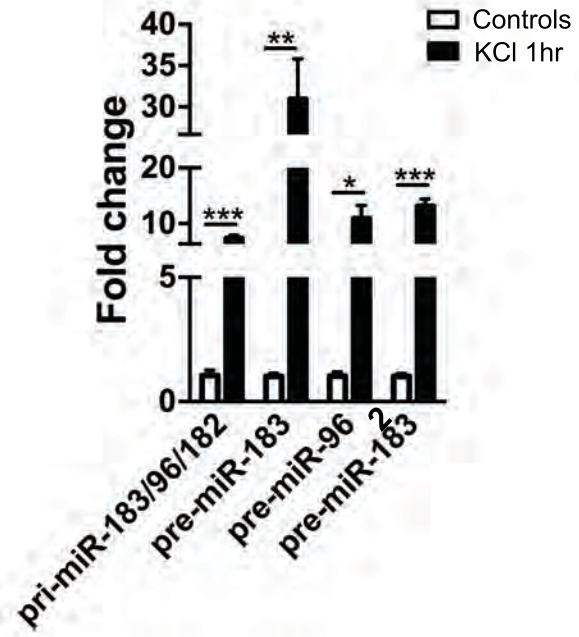

d

Cytoplasmic fraction

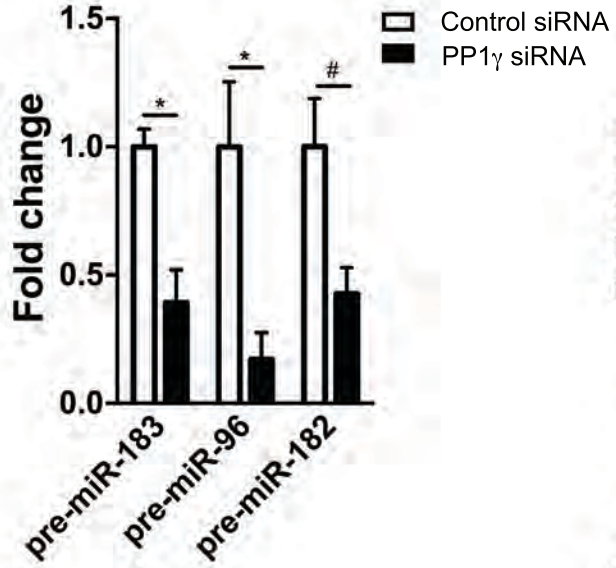

e

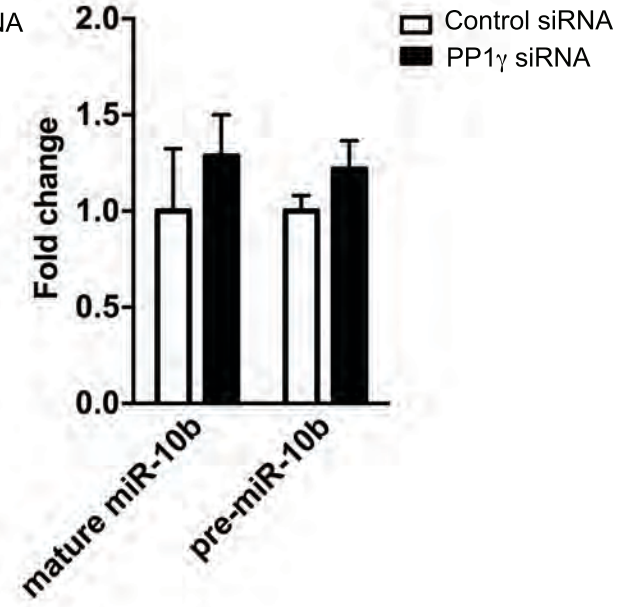

Supplementary Figure 6: Effect of PP1γ inhibition on miR-183/96/182 precursor and mature transcripts in N2A cells. (a) Representative Western blot of PP1γ in whole cell extracts of N2A cells transfected with PP1γ siRNA (left panel), and quantification of blots (right panel, t4=4.31, *p<0.05). (b) Mature miR-183/96/182 expression in N2A cells (whole cells fraction) afterPP1γ knockdown (miR-183: t4=3.26, *p<0.05; miR-96: t4=0.28, p=0.8; miR-182: t4=2.33, #p=0.08). (c) Pri-miR-183/96/182 and pre-miR-183/96/182 expression in whole cell extract of N2A cells after 1hr KCl stimulation (pri-miR-183/96/182: t4=4.31, ***p<0.001; pre-miR-183: t4 =6.13, **p<0.01; pre-miR-96: t4 =4.20, *p<0.05; pre-miR-182: t4=9.26, ***p<0.001).
(d) Cytoplasmic pre-miR-183/96/182 level in N2A cells after PP1γ knockdown and 1hr KCl stimulation (pre-miR-183: t4=4.16, *p<0.05; pre-miR-96: t4=3.02, *p<0.05; pre-miR-182: t4=2.68, #p=0.06). (e) Level of mature (t4=1.29, p=0.27) and precursor (t4=0.73, p=0.50) transcripts of miR-10b in cells treated with PP1γ siRNA. Bar graphs represent mean ± s.e.m.

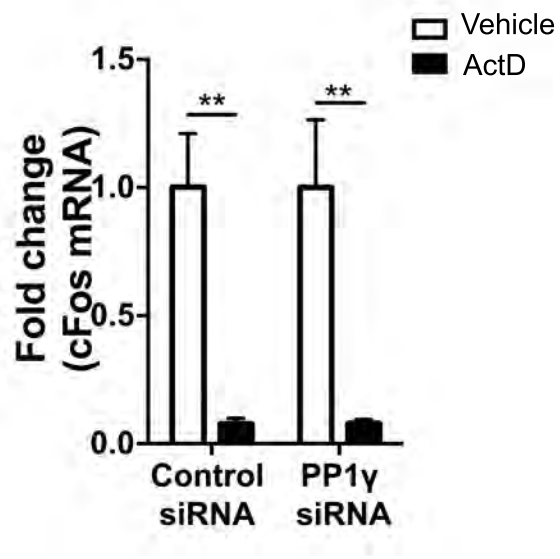

Supplementary Figure 7: Verification of Actinomycin D treatment on c-Fos expression in N2A cells treated with KCl for 1hr; (Two-way ANOVA, ActD- $F_{1,8}=29.77$, $p=0.0006$. post-hoc: Control siRNA $t_8=3.86$, $^{**}p<0.01$; PP1γ siRNA: $t_8=3.86$, $^{**}p<0.01$). Bar graphs represent mean ± s.e.m.

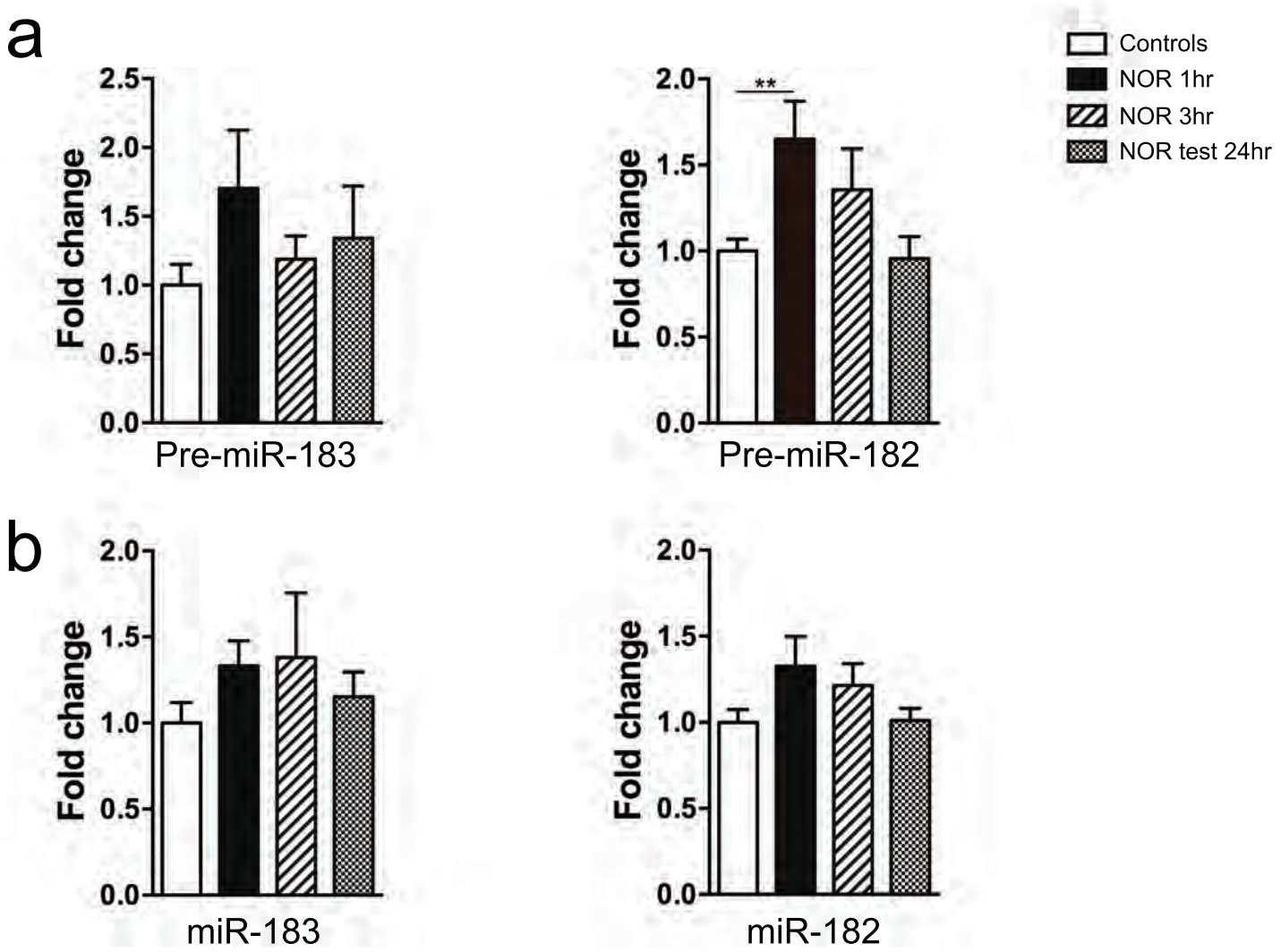

Supplementary Figure 8: MiRNA expression in hippocampus of mice trained with the strong NOR protocol and sacrificed at 1h, 3hr or 24hr after testing. (a) Left panel: pre-miR-183 one-way ANOVA $F_{3,23} = 1.16$, $p=0.35$; right panel: pre-miR-182 one-way ANOVA $F_{3, 23} = 4.00$, $p=0.02$, posthoc (control, NOR 1hr) $^{**}p<0.01$). (b) Left panel: miR-183 one-way ANOVA $F_{3, 23} = 0.78$, $p=0.51$; right panel: miR-182 one-way ANOVA $F_{3, 23} = 2.00$, $p=0.14$. Bar graphs represent mean ± s.e.m.

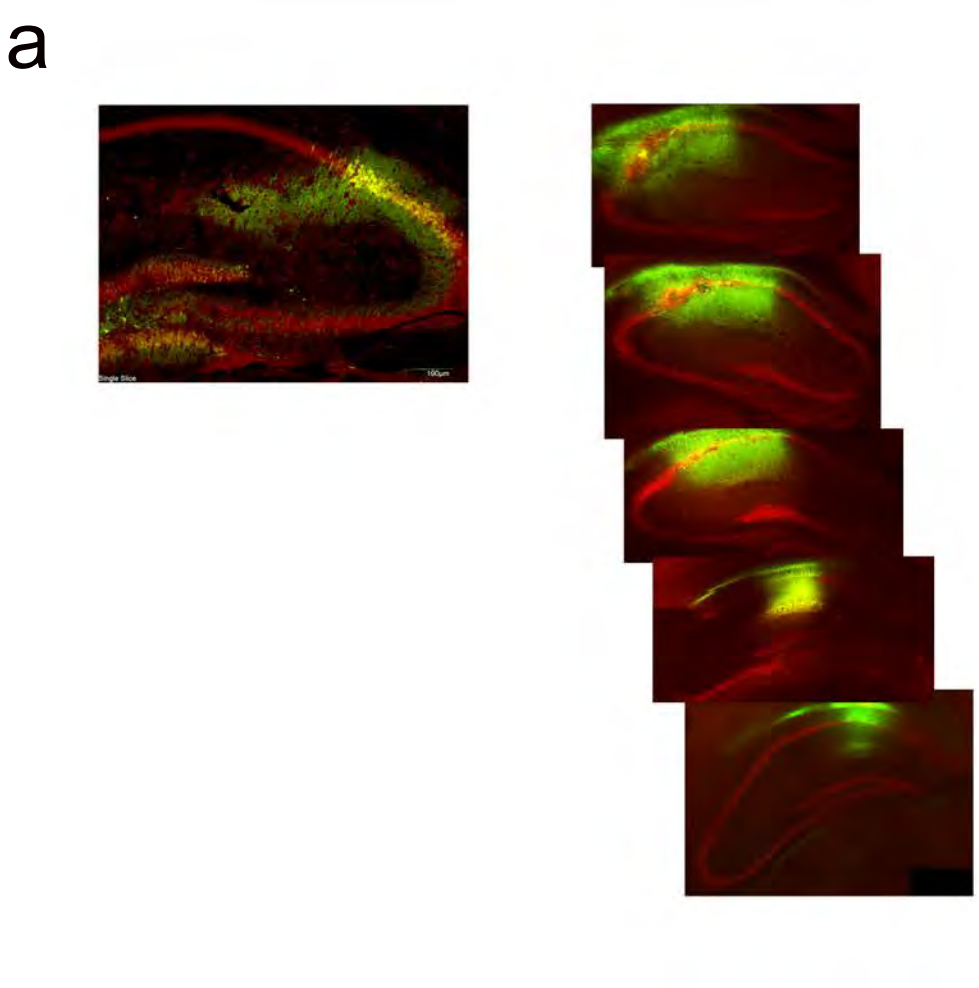

Supplementary Figure 9: AAV-mediated expression of miR-183/96/182 in the mouse hippocampus. (a) GFP staining of a brain slice 21 days after injection of a scAAV-cluster 183-GFP virus into the hippocampus. Neurons are labeled in red and GFP-expressing cells are green (anti-GFP). The series of images shown on the right panel display the extent of spread in the antero-posterior direction. (b) qPCR measurement of mature miR-183/96/182 levels in mouse hippocampus after injection with scAAV-control-GFP or scAAV-cluster 183-GFP (miR-183: t4=10.53, ***p<0.001; miR-96, t4=9.43, ***p<0.001; miR-182, t4=14.58, ***p<0.001; miR-10b, t4=0.55, p=0.61; controls, n=3; miR-183/96/182, n=3). Bar graphs represent mean ± s.e.m.

a

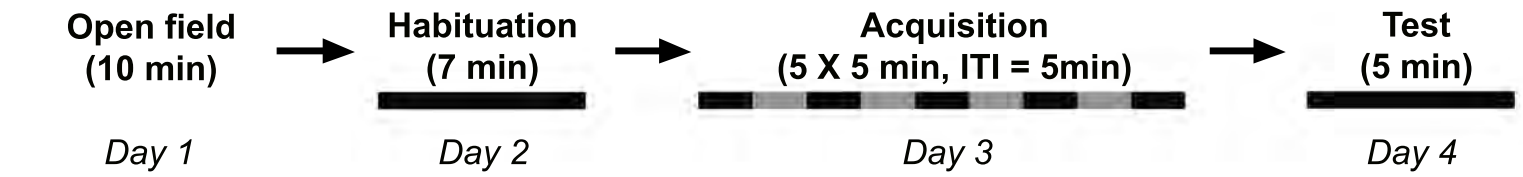
Open field
(10 min)
Habituation
(7 min)
Acquisition
(5 X 5 min, ITI = 5min)
Test
(5 min)
Day 1
Day 2
Day 3
Day 4

b

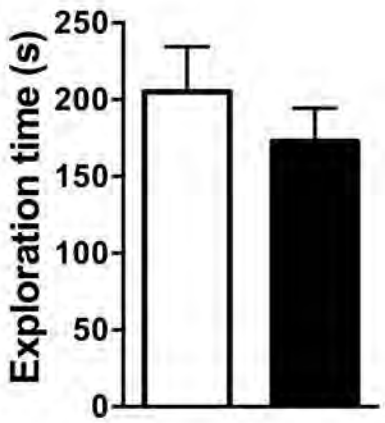
Exploration time (s)
250
200
150
100
50
0
Time spent on
novel object

c

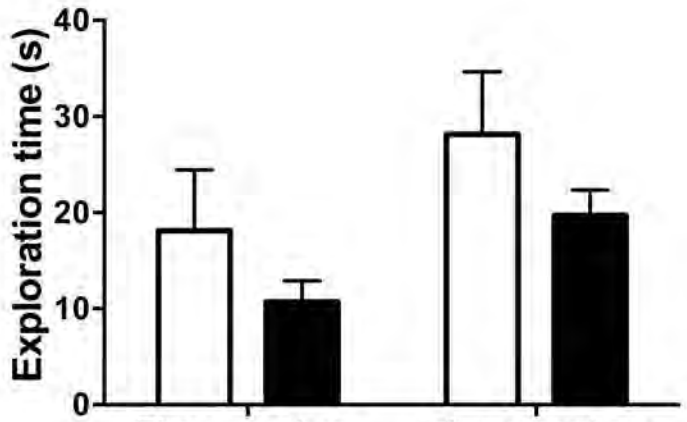
Exploration time (s)
40
30
20
10
0
Time spent on
all objects

d

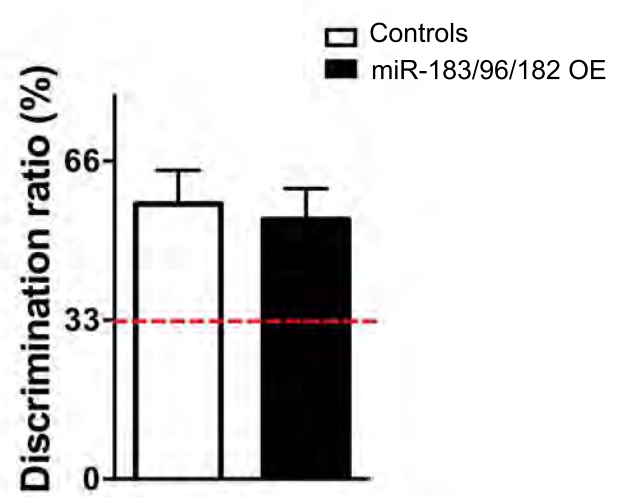
Controls
miR-183/96/182 OE
Discrimination ratio (%)
66
33
0

e

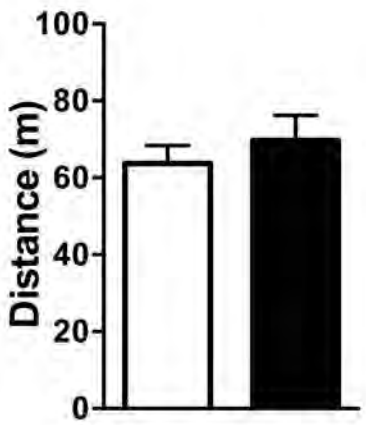
Distance (m)
100
80
60
40
20
0

f

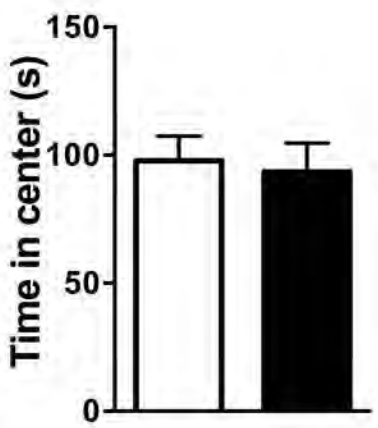
Time in center (s)
150
100
50
0

Supplementary Figure 10: MiR-183/96/182 overexpression (miR-183/96/182 OE) in the hippocampus does not influence long-term object memory with a strong training protocol. (a) Experimental setup. (b, c) Time spent exploring objects during acquisition (b, $t_{10}=0.88$, $p=0.40$), and testing on the NOR task (c, time on novel object: $t_{10}=1.1$, $p=0.29$; time on all objects: $t_{10}=1.2$, $p=0.26$) (d) Discrimination ratio of novel object over familiar objects (one-sample t-test, control: $t_5=3.43$, $p<0.05$; miR-183/96/182 - $t_5=3.27$, $p<0.05$; unpaired t test between controls and miR-183/96/182: $t_{10}=0.34$, $p=0.74$); the broken line shows chance level of discrimination set at 33%. (e, f) Total distance covered ($t_{10}=0.75$, $p=0.47$) (e), and total time spent in the center of the arena ($t_{10}=0.30$, $p=0.77$) (f), during open field-testing showing similar performance in control and miR-183/96/182 overexpressing mice. Controls, n=6; miR-183/96/182 OE, n=6. Bar graphs represent mean ± s.e.m.

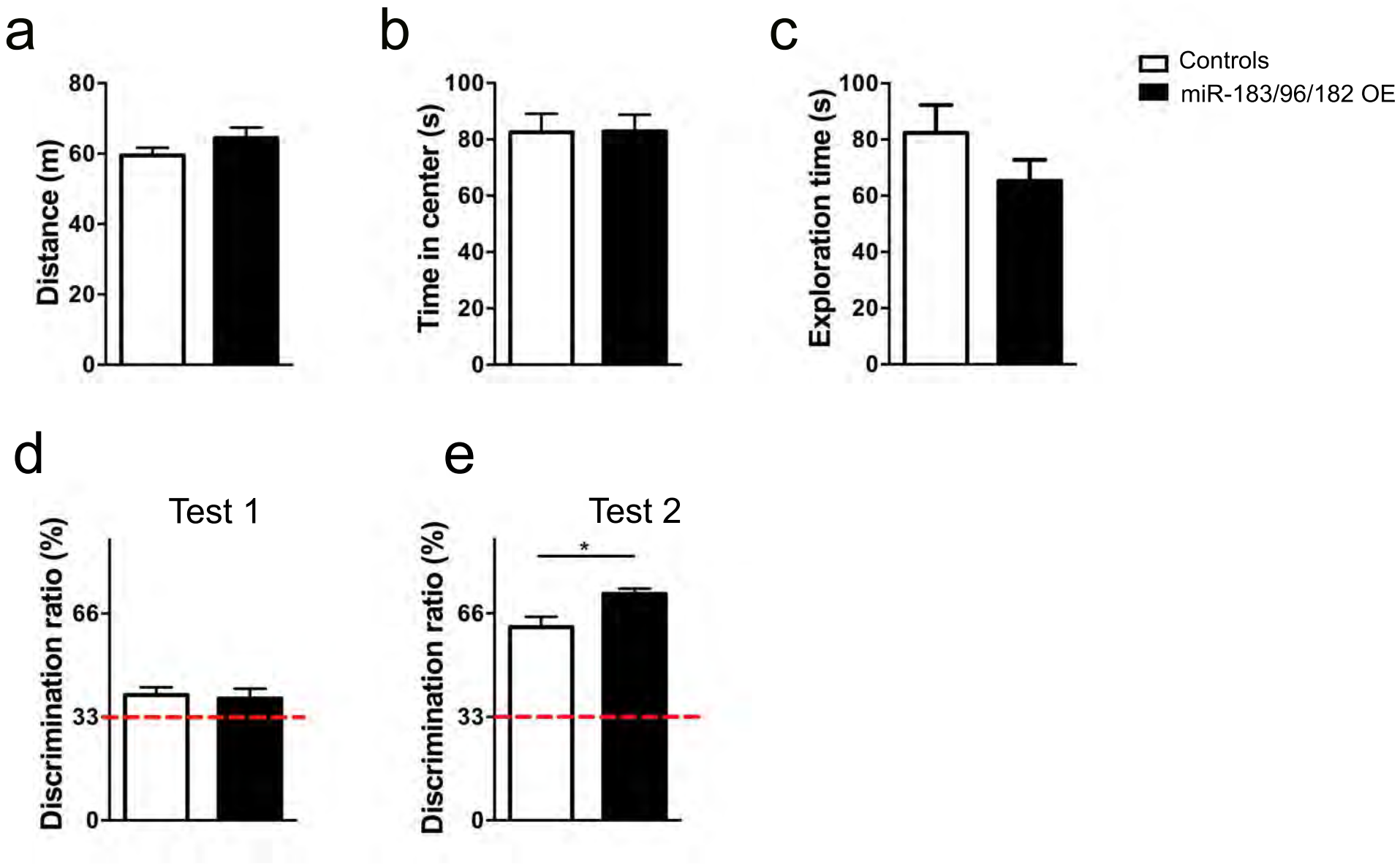

Supplementary Figure 11: Performance of miR-183/96/182 expressing (miR-183/96/182 OE) mice and controls in a weak training protocol. (a) Total path length during open field test ($t_{32}=1.30$, $p=0.20$); (b) Time spent in the center of the arena during open field test ($t_{32}=0.04$, $p=0.97$); (c)Time spent exploring objects during acquisition ($t_{32}=1.32$, $p=0.197$). (d) Discrimination ratio during test 1, 24hr after NOR training (One sample t-test, controls: $t_{18}=2.86$, $p<0.05$; miR-183/96/182, $t_{14}=1.84$, $p<0.1$); unpaired t-test between group comparison: ($t_{32}=0.3$, $p=0.77$). (e) Discrimination ratio during test 2, 48hr after NOR training (One sample t-test, control: $t_{18}=8.82$, $p<0.001$; miR-183/96/182: $t_{14}=22.37$, $p<0.001$); unpaired t-test between group comparison ($t_{32}=2.65$, $^*p<0.05$). Controls, n=19; miR-183/96/182 OE, n=15. Bar graphs represent mean ± s.e.m.

a

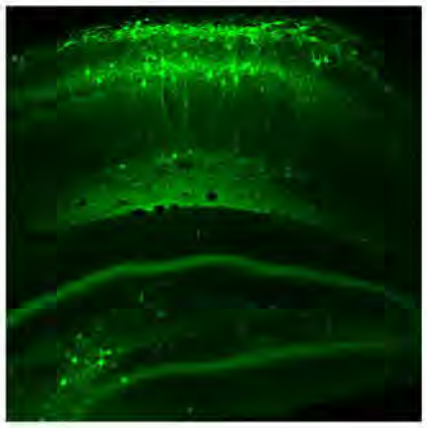

b

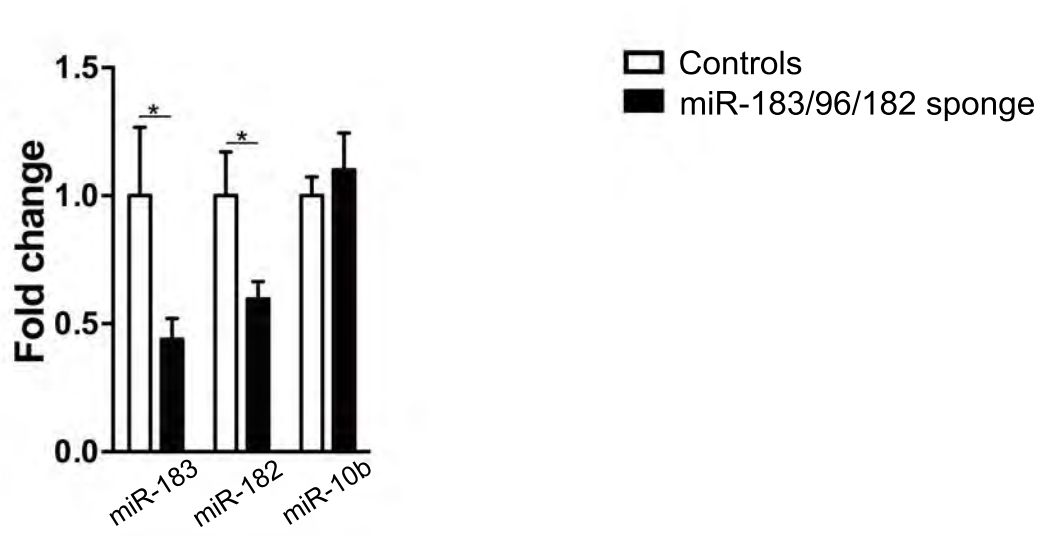
Controls
miR-183/96/182 sponge
Fold change
1.5
1.0
0.5
0.0
*
*
miR-183
miR-182
miR-10b

c

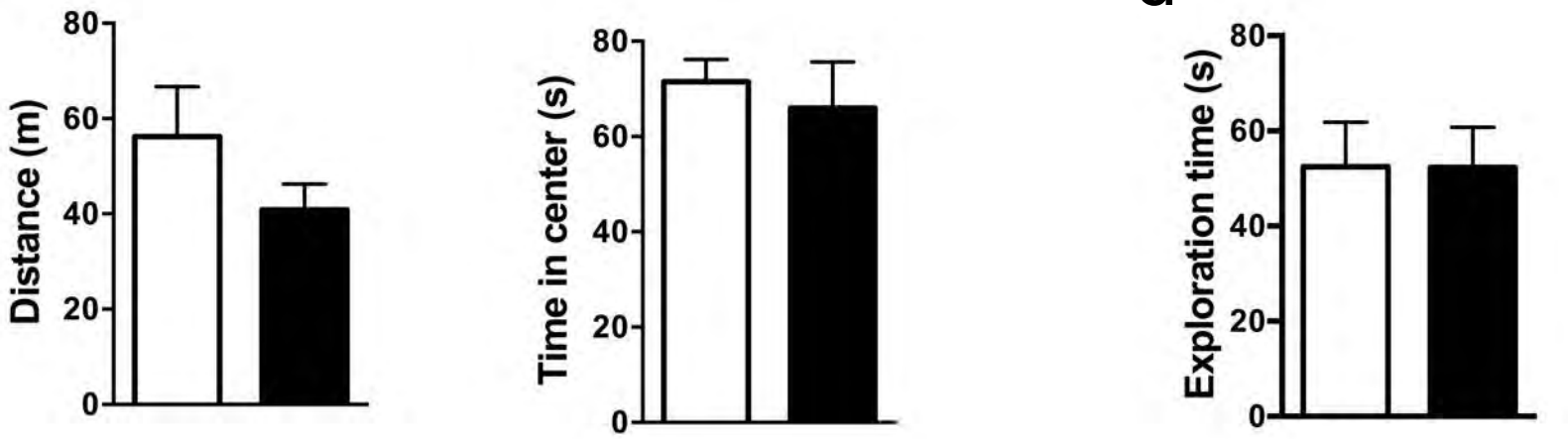
Distance (m)
80
60
40
20
0
Time in center (s)
80
60
40
20
0
Exploration time (s)
80
60
40
20
0

e

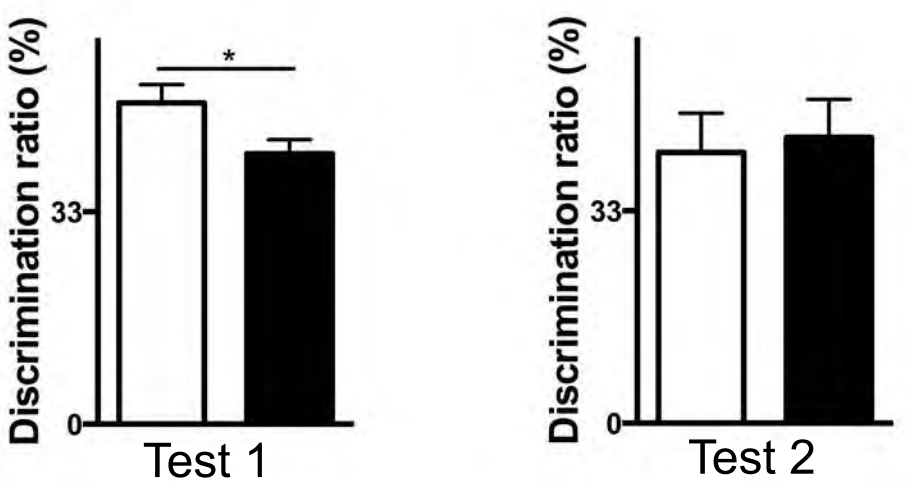
Discrimination ratio (%)
*
33
0
Test 1
Discrimination ratio (%)
33
0
Test 2

Supplementary Figure 12. Performance of mice expressing miR-183/96/182 sponge in the hippocampus under the weak NOR paradigm. (a) GFP expression in CA1 area of the hippocampus 10 days after scAAV-hSyn-miR-183 cluster sponge injection. (b) Quantification of miRNA expression in the hippocampus of mice expressing the sponge construct 30 days after virus injection (miR-183: $t_{14}=2.23$, $^*p<0.05$; miR-182: $t_{14}=2.40$, $^*p<0.05$; miR-10b: $t_{14}=0.57$, $p=0.58$); Control, n=7, miR-183/96/182, n=9. (c) Total distance covered (left panel: $t_{18}=1.31$, $p=0.21$) and time spent in center arena (right panel: $t_{18}=0.52$, $p=0.609$) during open-field test. (d) Total object exploration during 10min acquisition session ($t_{18}=0.01$, $p=0.99$). (e) Discrimination ratio 24hr (test 1: $t_{17}=0.25$, $^*p<0.5$) and 48hr (test 2, $t_{16}=0.28$, $p=0.78$) after NOR training. Control, n=9-10; miR-183/96/182 sponge, n=9-10). Bar graphs represent mean ± s.e.m.

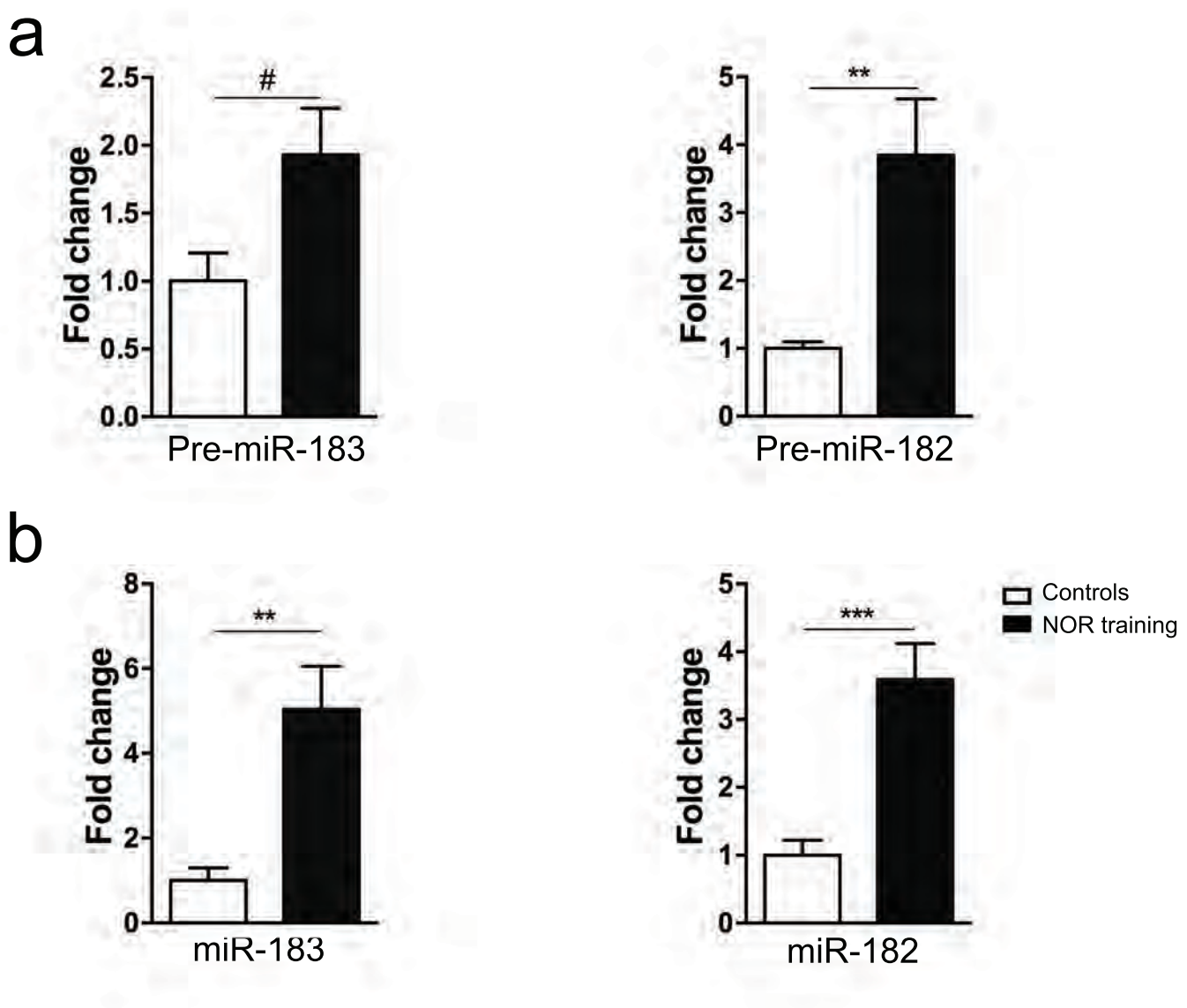

Supplementary Figure 13: Hippocampal miRNA expression 30 minutes after training with the weak NOR protocol. (a) Left panel: pre-miR-183, t6=2.32, #p=0.06; right panel: pre-miR-182, t7=3.01, *p=0.02. (b) Left panel: miR-183, t9=4.15, **p<0.01; right panel: miR-182, t9=4.8, ***p≤0.001. Control, n= 4-6; NOR, n=5. Bar graphs represent mean ± s.e.m.

a

b

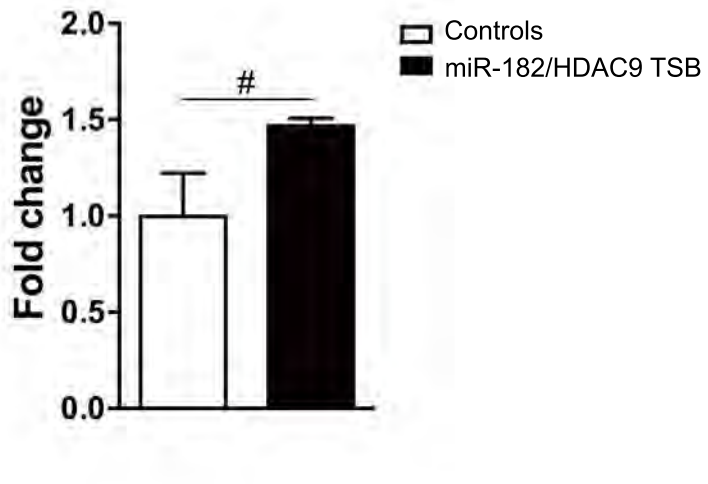

Supplementary Figure 14: miR-182/HDAC9 target site blocker (TSB) and its effect on HDAC9 expression. (a) Alignment of miR-182 TSB at HDAC9 3'UTR; sequences labeled in red are miR-182 seed sequence binding sites. (b) HDAC9 mRNA level in N2A cells treated with miR-182 TSB (t_6=2.05, #p=0.087). Bar graphs represent mean ± s.e.m.

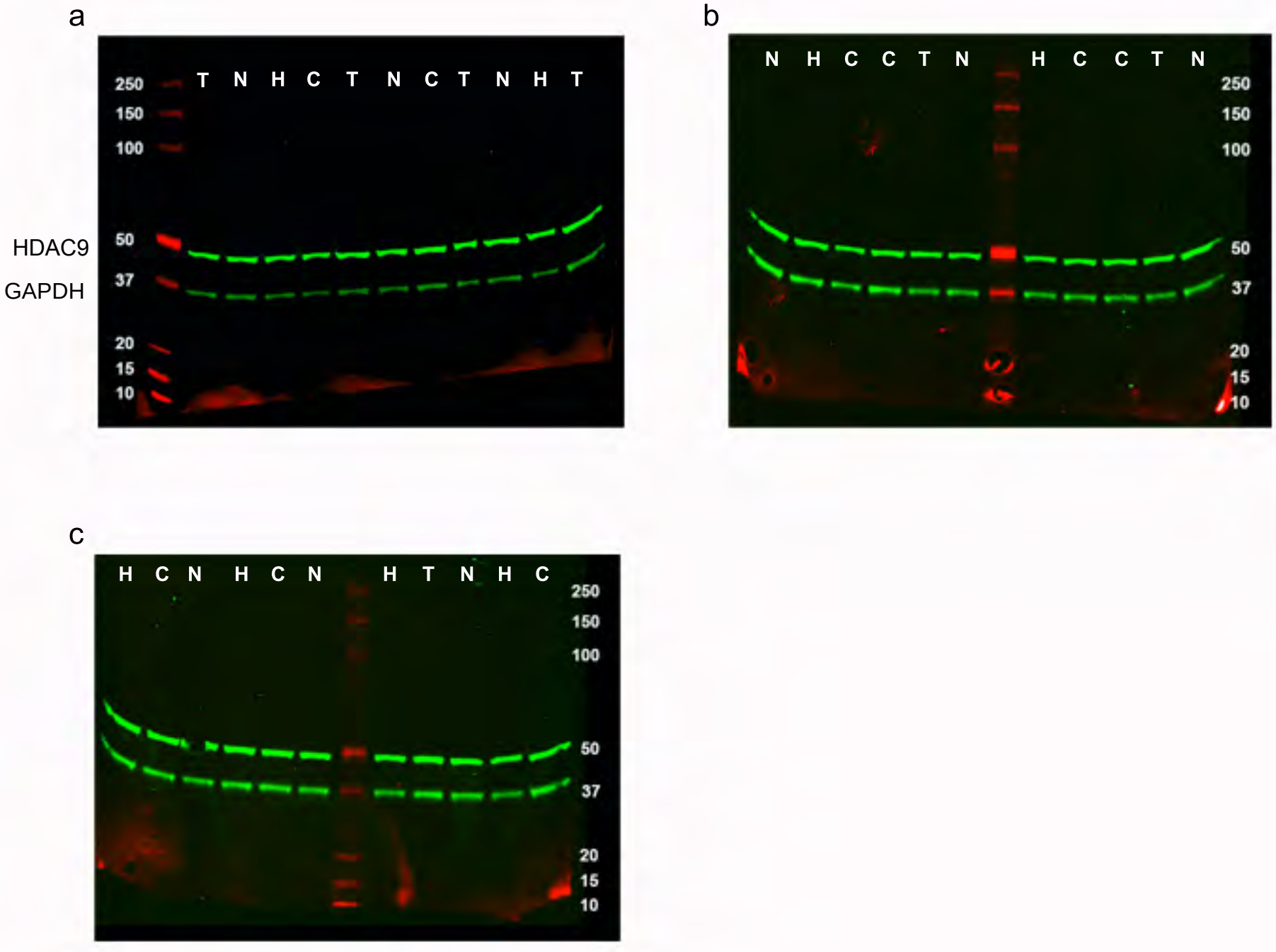

Supplementary Figure 15: Western blots for HDAC9 and GAPDH on hippocampal extracts (a-c). The numbers on the sides refer to molecular weight of the marker. C: cage control, H: habituation only, N: NOR training, T: training and test.

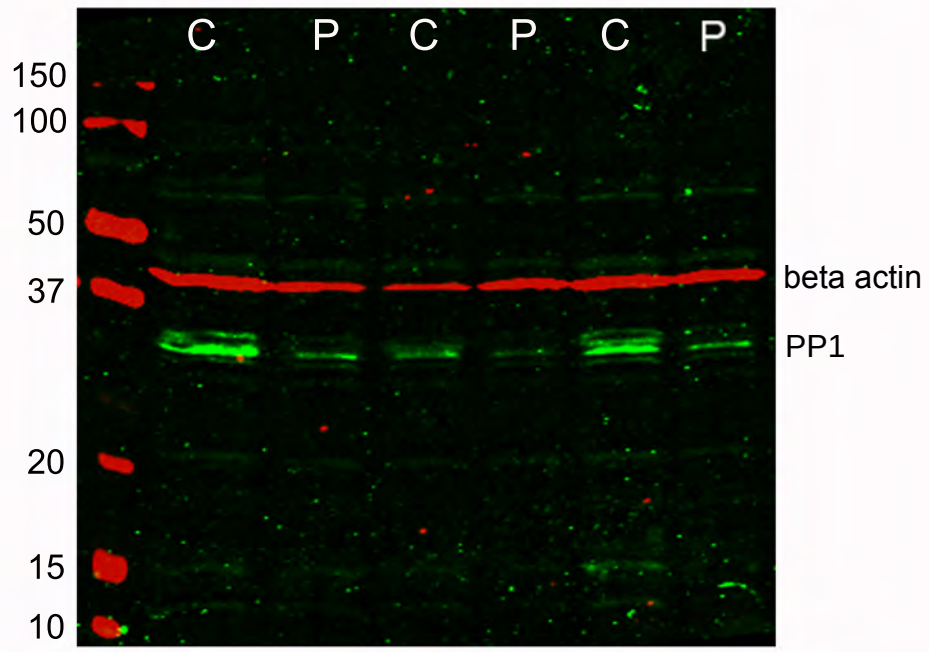

Supplementary Figure 16: Western blots for PP1 and beta actin on whole cell lysate from N2A cells transfected with PP1g siRNA (P) or scrambled control siRNA (C). The numbers on the side indicate molecular weight of the marker.

(a)

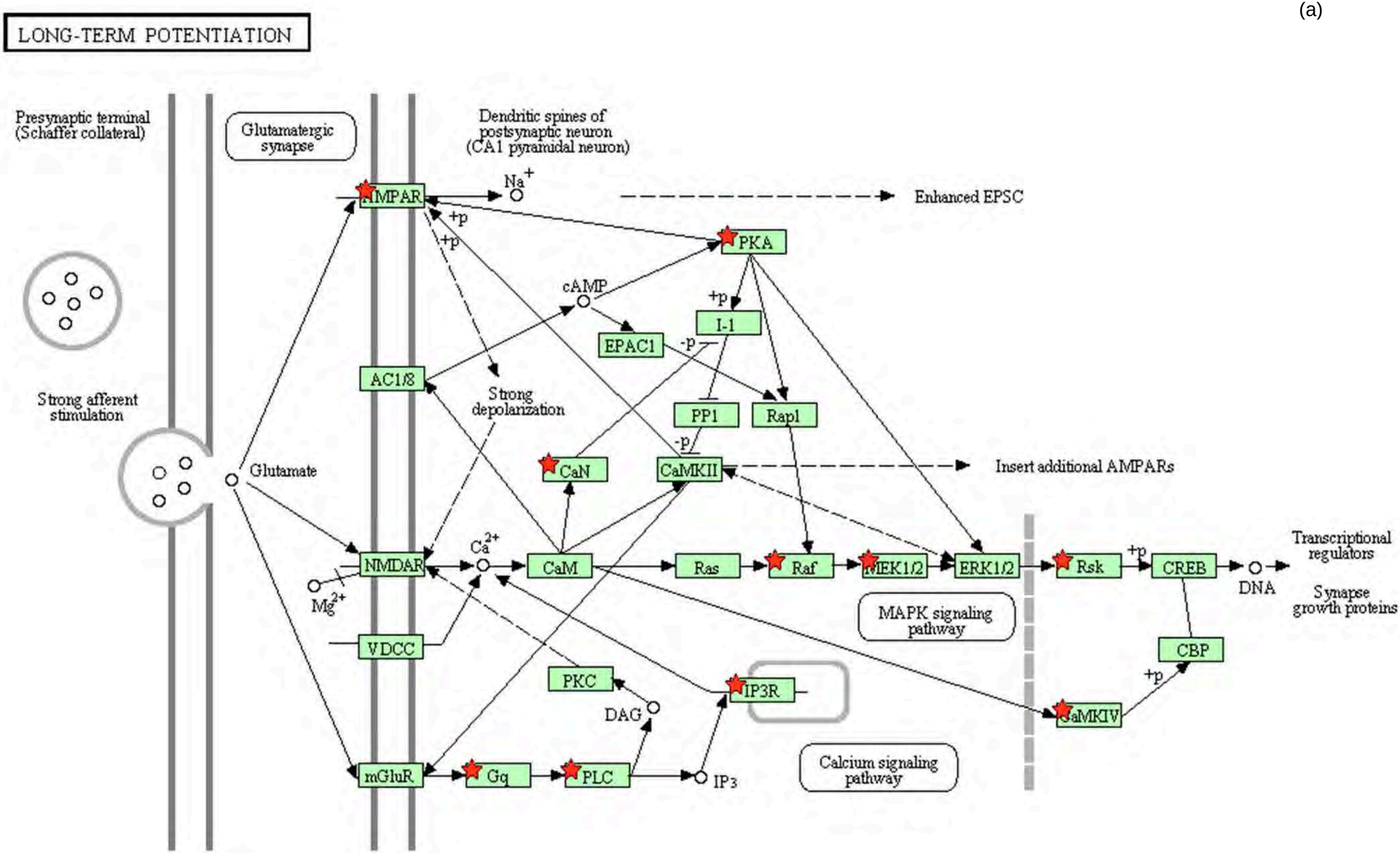
LONG-TERM POTENTIATION
Presynaptic terminal (Schaffer collateral)
Glutamatergic synapse
Dendritic spines of postsynaptic neuron (CA1 pyramidal neuron)
Strong afferent stimulation
Glutamate
AMPAR
Na+
Enhanced EPSC
+p
+p
PKA
cAMP
+p
I-1
EPAC1
-p
AC1/8
Strong depolarization
PP1
Rap1
-p
CaN
CaMKII
Insert additional AMPARs
NMDAR
Ca2+
CaM
Ras
Raf
MEK1/2
ERK1/2
Rsk
+p
CREB
DNA
Transcriptional regulators
Synapse growth proteins
Mg2+
MAPK signaling pathway
VDCC
CBP
+p
PKC
IP3R
DAG
CaMKIV
mGluR
Gq
PLC
IP3
Calcium signaling pathway

(b)

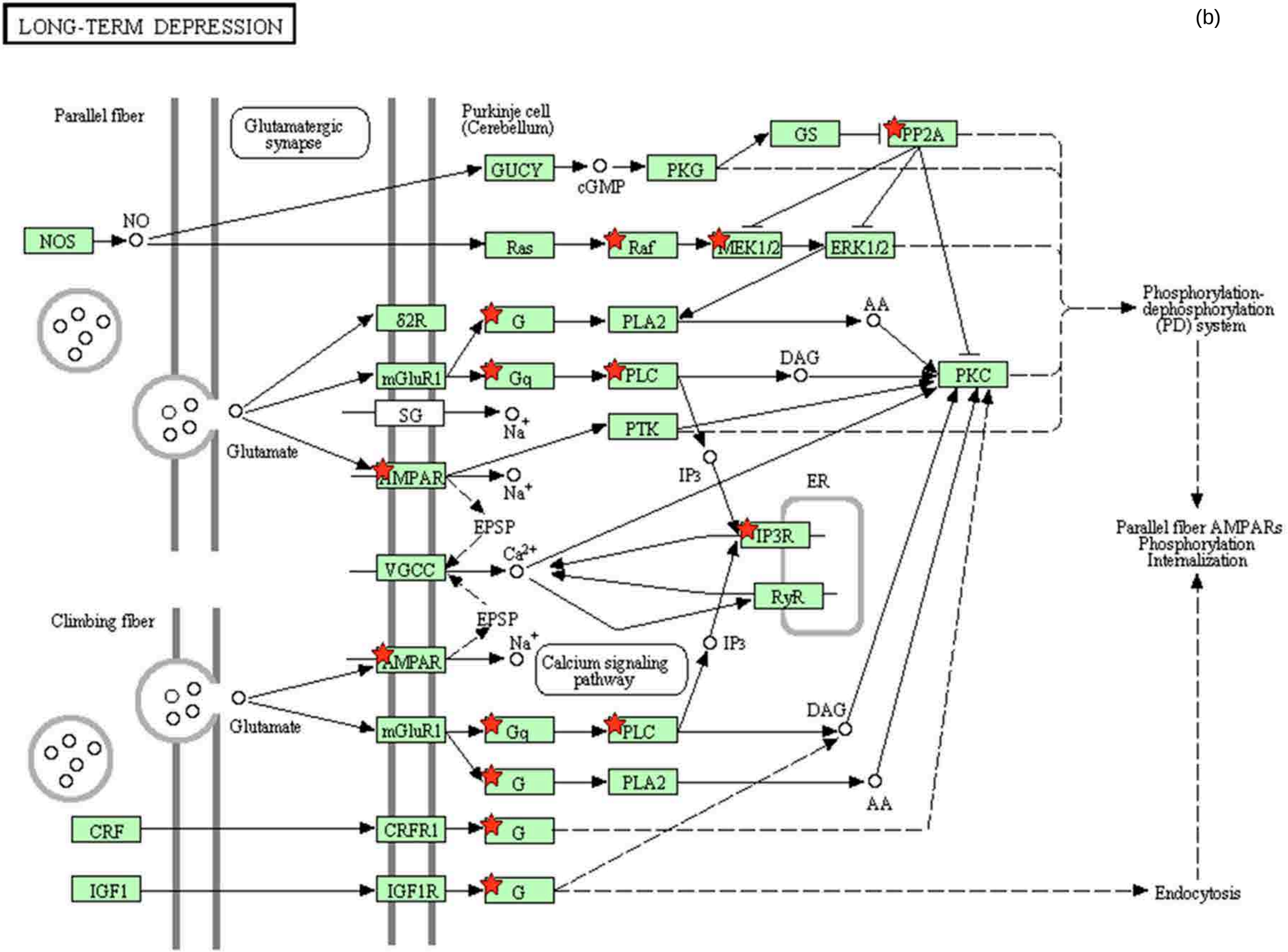
LONG-TERM DEPRESSION
Parallel fiber
Glutamatergic synapse
Purkinje cell (Cerebellum)
GUCY
cGMP
PKG
GS
PP2A
NO
NOS
Ras
Raf
MEK1/2
ERK1/2
δ2R
G
PLA2
AA
mGluR1
Gq
PLC
DAG
PKC
SG
Na+
PTK
Glutamate
AMPAR
IP3
ER
IP3R
EPSP
Ca2+
VGCC
RyR
Climbing fiber
Calcium signaling pathway
CRF
CRFR1
IGF1
IGF1R
Phosphorylation-dephosphorylation (PD) system
Parallel fiber AMPARs Phosphorylation Internalization
Endocytosis

(c)

MAPK SIGNALING PATHWAY

Classical MAP kinase pathway

JNK and p38 MAP kinase pathway

ERK5 pathway

Phosphatidylinositol signaling system

Heterotorimeric G-protein

IP3

cAMP

DAG

Ca^{2+}

CACN

PKA

Rap1

RasGRF

RasGRP

CNrasGEF

PKC

RafB

Raf1

Mos

NGF

BDNF

NT3/4

TrkA/B

EGF

FGF

PDGF

EGFR

FGFR

PDGFR

GRB2

SOS

Ras

G12

Gap1m

NF1

p120GAP

NIK

IKK

NFκB

Proliferation, inflammation anti-apoptosis

Scaffold

MP1

MEK1

MEK2

ERK

PTP

MKP

Tau

STMN1

cPLA2

MNK1/2

RSK2

CREB

Elk-1

Sap1a

c-Myc

SRF

DNA

c-fos

DNA

Proliferation, differentiation

PPP3C

GSTπ

HSP72

Evi1

FLNA

JIP3

ARRB

CrkII

NFAT-2

NFAT-4

GLK

HGK

Tpl2/Cot

Scaffold

MEKK1

HPK1

MLK3

Cdc42/Rac

PAK1/2

MEKK2/3

MKK4

MKK7

JIP1/2

JNK

PP2CA

AKT

LZK

MUK

MLTK

ASK2

ASK1

TAK1

PP2CB

PP5

MKK3

MKK6

p38

c-JUN

JunD

DNA

ATF-2

Elk-1

p53

p53 signaling pathway

Proliferation, differentiation, inflammation

Apoptosis

Cell cycle

Sap1a

GADD153

MAX

MEF2C

DNA

PRAK

MAPKAPK

MSK1/2

Cdc25B

HSP27

CREB

Serum, cytotoxic drugs, irradiation, heatshock, reactive oxygen species, lipopolysaccharide, and other stress

CASP

MST1/2

TRAF2

GCK

TNF

IL1

FASL

TGFB

LPS

TNFR

IL1R

FAS

TGFBR

CD14

DAXX

TAB1

TAB2

ECSIT

TRAF6

DNA damage

GADD45

MEKK4

MAO1/2

NLK

Wnt signaling pathway

Serum, EGF, reactive oxygen species, or Src tyrosinkinase downstream

MEK5

ERK5

Nur77

DNA

Proliferation, differentiation

MAPKKKK

MAPKKK

MAPKK

MAPK

Transcription factor

(d)

NEUROTROPHIN SIGNALING PATHWAY

Neuron

MAPK signaling pathway

NGF
BDNF
NT4
NT3
TrkA
TrkB
TrkC
ARMS
FRS2
Crk
C3G
Rap1
B-Raf
MEKK3
MEK5
Erk5
p38
MAPKAPK2
homo/heterodimers
rAPS
SH2B
GRB2
SOS
Ras
Raf
MEK1/2
Erk1/2
SH-PTP2
cAbl
Shc
Gab1
PI3K
PIP3
PDK
Akt
IRS1
CHK
Ubiquitin mediated proteolysis
IκB
NFκB
DNA
Retrograde transport
FKHRL1
FasL
Cell survival
PLCγ
DAG
PKCδ
Bad
GSK3β
IP3
Ca2+
CaM
CaMK
CREB
Plasticity
Long-term potentiation
ceramide
RhoGDI
RhoA
Regulation of actin cytoskeleton
Membrane ruffling
Axonal outgrowth
Axonal guidance
Axon patterning
Synapse formation
p75βP
p75ICD
PSEN
γ-secretase
extracellular domain
p75CTF
SC-1
NRAGE
Cell cycle arrest
TRAF6
NRIF
p73
p53
Bax
Apoptosis
p75NTR
Cdc42
Rac1
MEKK1
ASK1
MKK7
JNK
c-Jun
NADE
14-3-3ε
Sortilin
RIP2
IRAK
TRAF6
IKKβ
Cellular differentiation
Cell survival
Retrograde transport
Axonal outgrowth
p90RSK
MSK1
CREB
Bcl-2

(e)

REGULATION OF ACTIN CYTOSKELETON

LPS
F2
Chemotactic factor
INS
GF
FN1
Chemotactic factor
Bradykinin
Acetylcholine
F2RCD14
RTK
ITG
GPCR
Gα12,13
Sos
FAK
Cas
CrkII
Gβγ
FGD1/3
JNK, p38
MAPK signaling pathway
Gene expression
Raf
Ras
c-Src
Dock180
+p
MEK
PI3K
Rac1GEF
+p
ERK
PIP3
Vav/Tiam1
Actin polymerization
Adherens junction
IQGAP
Cdc42
Drf3
IRSp53
Mena
Arp2/3
F-Actin
N-WASP
Filopodia
+p
RhoGEF
GRLF1
Asef
APC
Rho
Rac
PIR121
Nap125
Abi2
HSPC300
WAVE1
TMSB4
PXN
GIT1
PIX
PFN
Actin polymerization
Focal adhesion assembly
ERM
NHE1
+p
+p
PAK
IRSp53
WAVE2
+p
VCL
ACTN
PIP2
PI4P5K
+p
ROCK
Focal adhesion
+p
+p
+p
+p
+p
mDia
MLCP
MLCK
PI4P5K
LIMK
+p
F-Actin
Arp2/3
CFN
Stabilization of actin
-p
+p
PFN
MLC
PIP2
-p
SSH
Lamellipodia
Actin polymerization stress fiber
?
Actomyosin assembly contraction
F-Actin
VCL
GSN
MyosinII
Focal complex assembly
Focal adhesion
Stress fibers

Supplementary Figure 17: Top pathways with predicted target genes of miR-183/182/96 cluster. Many predicted target genes (highlighted with red stars) are involved in regulation of long-term potentiation (a), long-term depression (b), MAPK signaling (c), neurotrophin signaling (d), and actin cytoskeleton (e). Target prediction and pathway analysis performed using mirPath and DAVID respectively and schematics was generated using KEGG pathway database.

Supplementary Table 1: List of primers, siRNAs, and plasmids

Primer/siRNA/plasmid	Source/sequence
miR-183, forward primer	Qiagen, cat. No.: MS00001722
miR-182, forward primer	Qiagen, cat. No.: MS00011291
miR-96, forward primer	Qiagen, cat. No.: MS00001456
miR-135a, forward primer	Qiagen, cat. No.: MS00011130
miR-135b, forward primer	Qiagen, cat. No.: MS00001575
miR-204-3p, forward primer	Qiagen, cat. No.: MS00024514
miR-146, forward primer	Qiagen, cat. No.: MS00001638
miR-200c, forward primer	Qiagen, cat. No.: MS00001827
Let-7c, forward primer	Qiagen, cat. No.: MS00005852
miR-190, forward primer	Qiagen, cat. No.: MS00032438
Pre-miR-10b, forward primer	Qiagen, cat. No.: MP00003983
miR-10b, forward primer	Qiagen, cat. No.: MS00032249
RNU6, forward primer	Qiagen, cat. No.: MS00033740
10X miScript Universal reverse primer	Qiagen, cat. No.: 218193
Pre-miR-96, forward & reverse primers	Qiagen, cat. No.: MP00006881
Pre-miR-183, forward & reverse primers	Qiagen, cat. No.: MP00004438
Pre-miR-182, forward & reverse primers	Qiagen, cat. No.: MP00004431
Pri-miR-183/96/182 forward	CCC TCC TAA AAC CAC CCT AA
Pri-miR-183/96/182 reverse	AGT TGG CAA GTC TAG AAC CAC
HDAC9, forward primer	ACG AGA AAG GGC AGT GGC AAG C
HDAC9, reverse primer	GAT GTG TGG TGG GCA GCC GT
NUFIP2, forward primer	AAC GCC GAA GAA GAA AAC AGG CTA
NUFIP2, reverse primer	GCT GAC ATC GGG ACC TGG GA
GAPDH, forward primer	CCA CTG GTG CTG CCA AGG CT
GAPDH, reverse primer	GGC AGG TTT CTC CAG GCG GC
Cacnb4, forward primer	TAC CTG CAT GGA GTT GAA GAC T
Cacnb4, reverse primer	TTC GCT CTC TCA AGC TGG ATA
Gabra1, forward primer	TGT GCG AGG GAG AGC AAG TC
Gabra1, reverse primer	AGC TAG GAA GCA GGG AGA TGT A
Prkcz, forward primer	GAC TGG GTG CAG ACA GAG AAA C
Prkcz, reverse primer	ACT CGA TGA CCA GGA ACA ACC G
18s rRNA, forward primer	CGGCTACCACATCCAAGGAA
18s rRNA, reverse primer	GCTGGAATTACCGCGGCT
Tubd1, forward primer	TCTCTTGCTAACTTGGTGGTCCTC
Tubd1, reverse primer	GCTGGGTCTTTAAATCCCTCTACG
Nrg1, forward primer	TGT GGT GGC CTA CTG CAA AA
Nrg1, reverse primer	TGG TGG GTT TGG ATG GTG AG
Ppp2ca, forward primer	ATG GAC GAG AAG TTG TTC ACC
Ppp2ca, reverse primer	CAG TGA CTG GAC ATC GAA CCT
Grm5, forward primer	CGT CTG GGG AAA CCC TAA GCT CCA
Grm5, reverse primer	TCA CCT CGA TGG CCG GCA GA
Gria1, forward primer	GTC CGC CCT GAG AAA TCC AG
Drosha, forward primer	GAG CCT AGA GGA AGC CAA ACA
Drosha, reverse primer	GCC GGA CGT GAG TGA AGA T
Dicer, forward primer	TTA ACC TTT TGG TGT TTG ATG AGT GT
Dicer, reverse primer	GCG AGG ACA TGA TGG ACA ATT
Ago2, forward primer	CCA TCT AGC TGT GAA GGC TCT GA
Ago2, reverse primer	TTC TTA GGG CCA GGC TTT AAA A
Gria1, reverse primer	CTC GCC CTT GTC GTA CCA C
Usp13, forward primer	CCC AGG GTA CAC GGG CCT GA
Usp13, reverse primer	GCT GAG GCT TGT GCT CCT CCT TC
Tubd1, forward primer	GGG AGA ATC ATG GAC CAG AA
Tubd1, reverse primer	TTG CTG CTG CTG TCT TTG TT
PP1γ siRNA pool	ON-TARGETplus Mouse Ppp1cc (19047) siRNA-SMARTpool, 5nmol. ThermoScientific catalog number L-040212-00-0005
Negative control siRNA	AllStars Negative control siRNA (20 nmol). Qiagen, catalog Number 1027281
PP1γ 3' UTR plasmid	Ppp1cc (GFP-tagged) - Mouse protein phosphatase 1, catalytic subunit, gamma isoform (cDNA clone MGC:13976 IMAGE:3487479), (10ug), 10µg. Origene, catalog number: MG204669

Supplementary Table 2: Results from t-tests, Fisher's LSD (protected or unprotected) and Tukey's posthoc analyses when appropriate.

Figure number	Description	t-test	One- or two-way ANOVA	Fisher's LSD posthoc	Tukey's posthoc
2c, left	Effect of PP1γ knockdown on pre-miR-183	Control vs PP1γ k/d t(4)=3.09, p=0.037	F(2,6)=3.12, p=0.12	t(6)=2.43, p=0.05	n/a
2c, middle	Effect of PP1γ knockdown on pre-miR-96	Control vs PP1γ k/d t(4)=3.75, p=0.02	F(2,6)=9.19, p=0.01	t(6)=3.83, p=0.009	n/a
2c, right	Effect of PP1γ knockdown on pre-miR-182	Control vs PP1γ k/d t(4)=3.52, p=0.02	F(2,6)=4.13, p=0.07	t(6)=2.82, p=0.03	n/a
2d	Effect of PP1γ knockdown on pri-miR-183/96/182		PP1 F(1,8)=5.37, p=0.049 ActD F(1,8)=35.62, p=0.0003	Vehicle t(8)= 3.30, p=0.01 ActD t(8)=0.02, p=0.99	Vehicle q(8)=4.66, p=0.04 ActD q(8)=0.02, p>0.99
2e, left	pre-miR-183 production with PP1 inhibition and ActD	Vehicle t(16)=3.47, p=0.004 ActD t(11)=2.53, p=0.028	PP1 F(1,27)=17.61, p=0.0003	Vehicle t(27)=3.13, p=0.004 ActD t(27)=2.85, p=0.008	Vehicle q(27)=4.43, p=0.02 ActD q(27)=4.02, p=0.04
2e, middle	pre-miR-96 production with PP1 inhibition and ActD	Vehicle t(16)=3.97, p=0.001 ActD t(27)=1.89, p=0.08	PP1 F(1,27)=16.13, p=0.0004	Vehicle t(27)=4.05, p=0.0004 ActD t(27)=1.80, p=0.078	Vehicle q(27)=5.73, p=0.002 ActD q(27)=2.59, p=0.28
2e, right	pre-miR-182 production with PP1 inhibition and ActD	Vehicle t(16)=4.80, p=0.0002 ActD t(12)=2.43, p=0.03	PP1 F(1,28)=21.3, p<0.0001	Vehicle t(28)=3.45, p=0.002 ActD t(28)=3.11, p=0.004	Vehicle q(28)=4.88, p=0.009 ActD q(28)=4.40, p=0.02
6c	HDAC9 protein level after NOR training	Cage control vs NOR testing t(14)=2.05, p=0.06 Habituation vs NOR testing t(13)=2.24, p=0.04	F(3,28)=2.06, p=0.13	Cage control vs NOR testing t(28)=2.20, p=0.036 Habituation vs NOR testing t(28)=1.99, p=0.05	n/a
Suppl. 7	Effect of ActD treatment on C-fos expression		ActD F(1,8)=29.77, p=0.0006	Control t(8)=3.86, p=0.0048 PP1γ k/d t(8)=3.86, p=0.0048	Control t(8)=5.46, p=0.02 PP1γ k/d t(8)=5.45, p=0.02
Suppl. 8a, left	Pre-miR-183 expression after training with strong NOR protocol		F(3,23)=1.16, p=0.35	n/a	n/a
Suppl. 8a right	Pre-miR-182 expression after training with strong NOR protocol		F(3,23)=4.00, p=0.02	Control vs NOR 1hr t(23)=2.97, p=0.007	Control vs NOR 1hr q(23)=4.20, p=0.03
Suppl. 8b, left	miR-183 expression after training with strong NOR protocol		F(3,23)=0.78, p=0.51	n/a	n/a
Suppl. 8b, right	miR-182 expression after training with strong NOR protocol		F(3,23)=2.00, p=0.14	n/a	n/a